



Average dynamics of a finite set of coupled phase oscillators

Germán C. Dima and Gabriel B. Mindlin

Citation: *Chaos: An Interdisciplinary Journal of Nonlinear Science* **24**, 023112 (2014); doi: 10.1063/1.4874015

View online: <http://dx.doi.org/10.1063/1.4874015>

View Table of Contents: <http://scitation.aip.org/content/aip/journal/chaos/24/2?ver=pdfcov>

Published by the [AIP Publishing](#)

Articles you may be interested in

[Phase and amplitude dynamics in large systems of coupled oscillators: Growth heterogeneity, nonlinear frequency shifts, and cluster states](#)

Chaos **23**, 033116 (2013); 10.1063/1.4816361

[Phase-flip transition in nonlinear oscillators coupled by dynamic environment](#)

Chaos **22**, 023147 (2012); 10.1063/1.4729459

[The dynamics of network coupled phase oscillators: An ensemble approach](#)

Chaos **21**, 025103 (2011); 10.1063/1.3596711

[Collective phase chaos in the dynamics of interacting oscillator ensembles](#)

Chaos **20**, 043134 (2010); 10.1063/1.3527064

[Experimental evidence of anomalous phase synchronization in two diffusively coupled Chua oscillators](#)

Chaos **16**, 023111 (2006); 10.1063/1.2197168



Re-register for Table of Content Alerts

Create a profile.



Sign up today!



Average dynamics of a finite set of coupled phase oscillators

Germán C. Dima^{a)} and Gabriel B. Mindlin

Laboratorio de Sistemas Dinámicos, IFIBA y Departamento de Física, Facultad de Ciencias Exactas y Naturales, Universidad de Buenos Aires, Pabellón 1, Ciudad Universitaria, Buenos Aires, Argentina

(Received 15 October 2013; accepted 18 April 2014; published online 2 May 2014)

We study the solutions of a dynamical system describing the average activity of an infinitely large set of driven coupled excitable units. We compared their topological organization with that reconstructed from the numerical integration of finite sets. In this way, we present a strategy to establish the pertinence of approximating the dynamics of finite sets of coupled nonlinear units by the dynamics of its infinitely large surrogate. © 2014 AIP Publishing LLC.

[<http://dx.doi.org/10.1063/1.4874015>]

Many fields of physics deal with the macroscopic description of large systems, composed by N interacting members. In some cases, it is possible to address them in terms of a mean field theory, designed to describe the parameters accounting for the average behavior of the system. This approach requires the study of a surrogate problem, consisting of an infinite number of interacting elements. In this work, we study the macroscopic dynamic of a system of N non-linear interacting units. For that, we use topological tools in order to compare the system of N units with its surrogate with infinite elements. We report, for a particular problem, a minimum number of units required for the two systems to be topologically equivalent.

I. INTRODUCTION

The study of nonlinearly coupled units has a long and rich history.¹ An important contribution to this field was a model introduced by Kuramoto,² which consists of a set of coupled oscillators, each one described in terms of its phase. In this model, the units are coupled through a sinusoidal function of the phase difference between the interacting units. Extensive work has been devoted to the study of this system.³ Recently, Ott and Antonsen showed that this model presents a stable invariant manifold in the limit of infinitely many units.⁴ In this way, it was shown that the average dynamics of the system can be described in terms of a low dimensional dynamical system. Strogatz made an in-detail analysis of a closely related set of equations (periodically forced Kuramoto model)⁵ as well as Antonsen *et al.*⁶ In all these approaches, the final results are reported in the limit of an arbitrarily large number of interacting units.

In many situations where a finite number of units are involved, an infinite limit is studied in order to gain an intuition on the expected dynamics. It is useful then to have tools that allow us to estimate the minimum size of a finite population such that its behavior can be approximated by a surrogate problem with infinite number of units. In this work, we

address this issue in the framework of a particular problem: The dynamics of a periodically driven set of coupled excitable elements. In the limit of infinitely many of them, the average dynamics of this system was shown to be described by a set of three ordinary differential equations.⁷ For three dimensional dynamical systems, there is a strategy that allows to establish the equivalence between flows: The topological equivalence between their periodic orbits.^{8–10} In this work, we analyze the solutions of the dynamical system describing the behaviour of the complex Kuramoto order parameter of an infinitely large set of driven, coupled, excitable units, for different parameters. Then we studied numerically finite size populations and compared the topological organization of the periodic solutions obtained in both systems.

II. THE MODEL

A modified version of the Kuramoto's model was previously studied by Alonso *et al.*¹¹ in order to describe the interaction of two sets of phase oscillators: One presenting periodic behavior and the other one, excitability. The dynamics of each unit is given by

$$\dot{\theta}_i^{(\sigma)} = \omega_i^{(\sigma)} - \gamma_i^{(\sigma)} \sin(\theta_i^{(\sigma)}) + \sum_{\sigma'=1}^2 \frac{K_{\sigma\sigma'}}{N^{(\sigma)}} \sum_{j=1}^{N^{(\sigma')}} \sin(\theta_j^{(\sigma')} - \theta_i^{(\sigma)}), \quad (1)$$

where σ indicates the different sets ($\sigma = 1$ driving set, $\sigma = 2$ driven set), the integers $i = 1, 2, \dots, N \triangleq (N^{(\sigma=1)} + N^{(\sigma=2)})$ index the oscillators, and $\omega_i^{(\sigma)}$ their natural frequency. The dynamics of each unit is described by its phase $\theta_i^{(\sigma)}(t)$. The parameter $\gamma_i^{(\sigma)}$ plays an important role in the dynamics of each uncoupled unit: all oscillators meeting the condition $|\omega_i^{(\sigma)} / \gamma_i^{(\sigma)}| \leq 1$ become an excitable oscillator. Finally, the parameter $K_{\sigma\sigma'}$ ($\sigma' = 1, 2$) denotes the coupling strength between populations. An order parameter is defined to measure the coherence of each set

$$z_\sigma = \frac{1}{N^{(\sigma)}} \sum_{j=1}^{N^{(\sigma)}} e^{i\theta_j^{(\sigma)}}. \quad (2)$$

In the $N \rightarrow \infty$ limit, the dynamics of the system can be described by a density probability function $f^{(\sigma)}(\theta, \omega, t)$,

^{a)} Author to whom correspondence should be addressed. Electronic mail: gdima@df.uba.ar

which is continuous over its variables. The complex order parameter of each set is now rewritten using this distribution

$$z_\sigma = \int_{-\infty}^{\infty} \int_0^{2\pi} e^{i\theta} f^{(\sigma)}(\theta, \omega, t) d\theta d\omega. \quad (3)$$

Assuming that the coefficients of the Fourier series of $f^{(\sigma)}(\theta, \omega, t)$ in θ can be expressed as $f_n^{(\sigma)}(\omega, t) = [\alpha_\sigma(\omega, t)]^n$ (Ott's ansatz⁴), and taking the natural frequencies of both

sets from a Lorentzian distribution $g^{(\sigma)}(\omega) = \frac{1}{\pi} \frac{\Delta^{(\sigma)}}{(\omega - \omega_0^{(\sigma)})^2 + (\Delta^{(\sigma)})^2}$, the order parameter can be written as $z_\sigma(t) = \alpha_\sigma^*(\omega_0^{(\sigma)} - i\Delta^{(\sigma)}, t)$. Here, $\omega_0^{(\sigma)}$ represents the median frequency and $\Delta^{(\sigma)}$ the spread of the distribution. We set $\gamma^{(1)} \equiv 0, K_{12} \equiv 0$ in order to describe the driving population. In this $N \rightarrow \infty$ limit, the system presents a low dimensional invariant manifold given by

$$\begin{cases} \dot{\alpha}_1 = -i(\omega_0^{(1)} - i\Delta^{(1)})\alpha_1 + \frac{K_{11}}{2}(1 - |\alpha_1|^2)\alpha_1 \\ \dot{\alpha}_2 = -i(\omega_0^{(2)} - i\Delta^{(2)})\alpha_2 + \frac{\gamma}{2}(1 - \alpha_2^2) + \frac{K_{21}}{2}(\alpha_1 - \alpha_1^*\alpha_2^2) + \frac{K_{22}}{2}(1 - |\alpha_2|^2)\alpha_2. \end{cases} \quad (4)$$

In order to simplify the notation, we wrote $\alpha_\sigma = \alpha_{(\sigma)}(\omega_0^{(\sigma)} - i\Delta^{(\sigma)}, t)$ and $\gamma^{(2)} \doteq \gamma$. For both populations, a complex notation is used for the order parameter $z_\sigma^*(t) = \alpha_\sigma = \rho_\sigma(t)e^{i\phi_\sigma(t)}$. We assume that the driving population presents a collective steady state, i.e., the magnitude of the order parameter is fixed. The whole problem, therefore, can be written as a 3D-system¹¹

$$\begin{cases} \rho_1 = \sqrt{1 - \frac{2\Delta^{(1)}}{K_{11}}} \\ \dot{\phi}_1 = -\omega_0^{(1)} \\ \dot{\rho}_2 = -\Delta^{(2)}\rho_2 + \frac{\gamma}{2}\cos(\phi_2)(1 - \rho_2^2) + \frac{K_{22}\rho_2}{2}(1 - \rho_2^2) + \frac{K_{21}\rho_1}{2}(1 - \rho_2^2)\cos(\phi_1 - \phi_2) \\ \rho_2\dot{\phi}_2 = -\omega_0^{(2)}\rho_2 - \frac{\gamma}{2}\sin(\phi_2)(1 + \rho_2^2) + \frac{K_{21}\rho_1}{2}(1 - \rho_2^2)\sin(\phi_1 - \phi_2). \end{cases} \quad (5)$$

III. RESULTS

Solutions of Eq. (5) were investigated numerically. Following previous works,¹¹ we set the parameters at values that allowed us to find a rich variety of solutions ranging from periodic to chaotic ones for the driven set order parameter $z_2(t)$.¹²⁻¹⁶ An Arnold's tongues diagram was obtained by varying the frequency of the driving set ($\omega_0^{(1)}$) and the

amplitude of its forcing to the excitable population (K_{21}). In this phase space, we searched for orbits of periods 1, 2, 3, 4, and 5. The regions of parameters space where the different solutions are found are color coded in Figure 1. All the tongues were labeled with the period number (in terms of the driving-set period) and a subscript number that allows to distinguish each tongue with the same period.

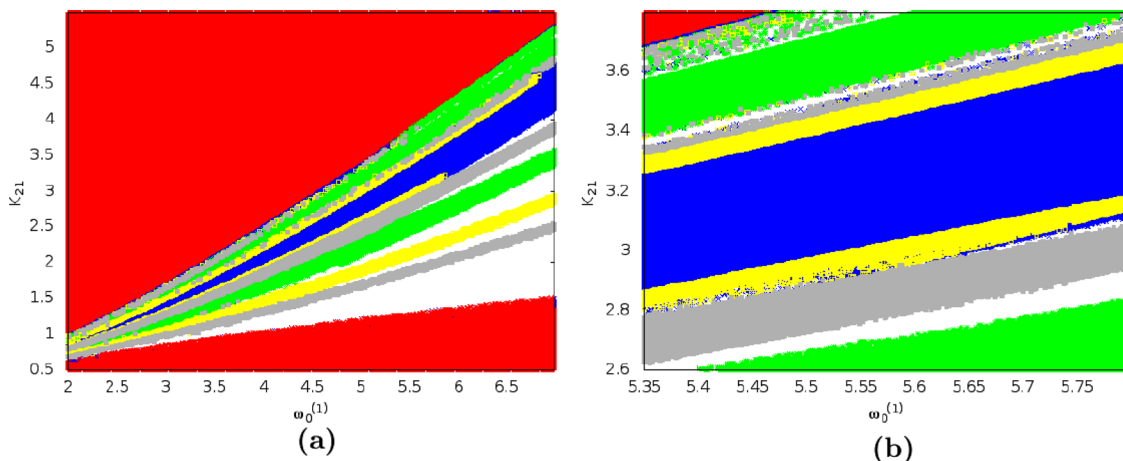


FIG. 1. (a) Arnold tongues diagram for the 3D-system. The fixed parameters used in our simulations are $\omega_0^{(2)} = 2.90, \Delta^{(1)} = \Delta^{(2)} = 1.00, \gamma = 2.96, K_{22} = 6.00,$ and $K_{11} = 8.00$. A central 2-periodic tongue (named 2_1 , blue) is enclosed by two tongues of period 4 (4_1 higher and 4_2 lower, in yellow). Another orbit of period 4 (4_3) appears between two tongues of period 5 (5_1 higher and 5_2 lower, in gray). Finally, two tongues of period 3 (3_1 higher and 3_2 lower) are shown in green. (b) Detail of the map.

A very interesting strategy was proposed by Gilmore and Lefranc¹⁰ in order to compare the flows generated by three dimensional non linear systems: The topological description of their periodic orbits.

Since the topological structure of the solutions obtained for parameters within each tongue is invariant, we selected a unique periodic orbit as a representative of the whole tongue where the orbit is found. There are many ways to characterize the topological features of periodic solutions of a three dimensional dynamical system: The way in which they link with other solutions, their knot types, etc. Among those stands, the relative rotation rates (*RRRs*), presented by Solari and Gilmore.¹⁷ For each pair of points (initial conditions) in the Poincaré section, the *RRR* describes the relative torsion between the trajectories starting from that pair of points at which the solutions meet the section. A positive/negative sign is added in the index, in order to indicate if the crossings of the curves obey the left-hand rule: clockwise twists are considered negative while counterclockwise twists are considered positive. These numbers applied to the same periodic orbit carry the name of self relative rotation rate (*SRRR*) and give information about deformations under the flow in the neighborhood of the orbit. The *RRR* and *SRRR* present robustness not only under coordinate transformations but also under changes in the control parameter as long as the orbits exist.

To compute these rates, we proceed as follows.¹⁰ The time series of the stationary state $A = Re(z_2(t))$ is plotted in a fixed time window corresponding to a full period τ . Then, a second copy of the periodic orbit (B) is made in the same plot, but shifted one period of the driving set (i.e., $B = Re(z_2(t +$

$\tau^{(1)})$ with $\tau^{(1)} = 2\pi/\omega_0^{(1)}$). Half of the sum of all crossings of both curves, over the number of periods of the driving set that fit in the window (i.e., $\tau/\tau^{(1)}$), is the relative rotation number for that pair of initial conditions in the Poincaré section. The standard notation of this index is $SRRR_{(1,2)}$, where the numbers label the initial conditions. The process is repeated using both $A = Re(z_2(t + (n - 1)\tau^{(1)}))$ and $B = Re(z_2(t + (m - 1)\tau^{(1)}))$, with $n, m = \{1, 2, \dots, \tau/\tau^{(1)}\}$ and $n < m$ (since $SRRR_{(n,m)} = SRRR_{(m,n)}$ and $SRRR_{(m,m)} = 0$ by definition). The set of *SRRR* for each orbit is obtained by counting the time each $SRRR_{(n,m)}$ is repeated, displayed as exponents. In Figure 2, we obtained $SRRR_{4_2} = (-\frac{1}{2})^8(-\frac{1}{4})^4 0^4$, meaning $(-\frac{1}{2})$ occurs 8 times while $(-\frac{1}{4})$ and 0 (corresponding to $RRR_{(m,m)}$) repeat four times each. In order to simplify the notation, only the ratios of the numbers are presented: $SRRR_{4_2} = (-\frac{1}{2})^4(-\frac{1}{4})^0$. The rationale behind this procedure is that all the crossings between the time series in the plot correspond to crossings in the bidimensional projection of the three dimensional phase space $Re(z), \frac{d}{dt}Re(z), t.mod(\tau_{driving})$. In this embedding, all crossings obey the left-hand rule resulting on negative indexes.

We test the hypothesis that, for a sufficiently large number of N phase oscillators, the topology of a set of periodic orbits in the complete system matches the topology of the averaged system. By fixing the parameters as in the averaged system, we compute the *SRRR* for solutions presented by sets of different number of oscillators (see Table I).

For $N = 500$ (the smallest set considered in our study), non periodic solutions were found at parameter values where the infinite system presented periodic solutions. Four

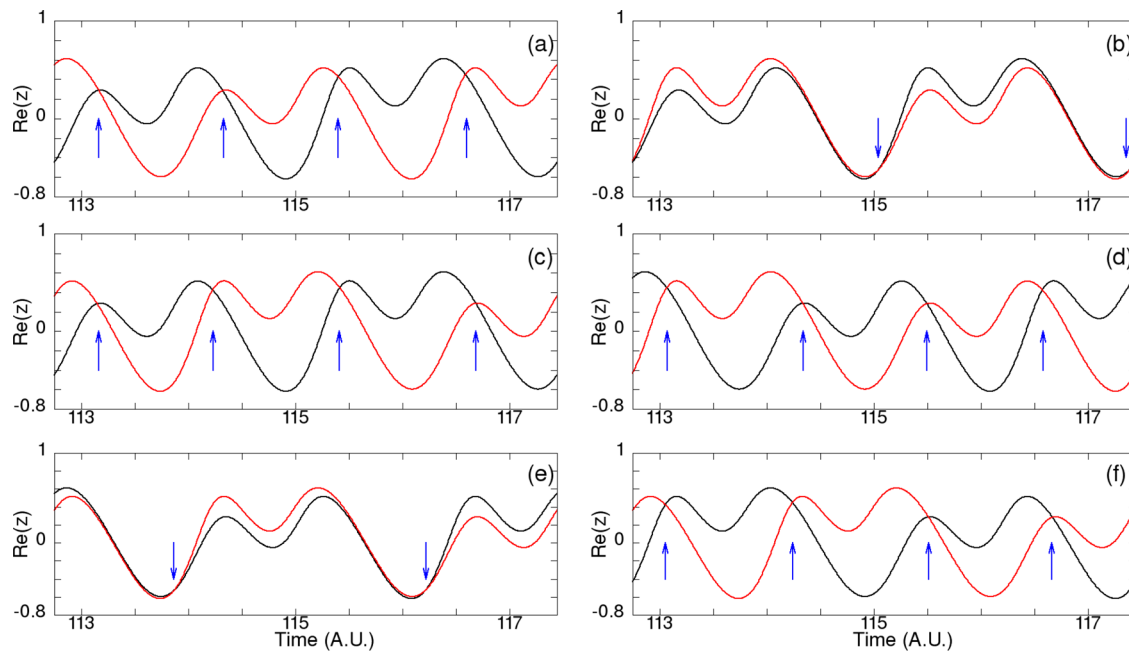


FIG. 2. Computing the *SRRR* of the orbit 4_2 in the averaged system by looking at the time series. (a) A full period of the temporal evolution of $Re(z_2)$ is plotted in a fixed window τ (black). Then the same plot is shifted by one driving-set period $\tau^{(1)}$ (red). The number of crossings (blue arrows) is counted. The *SRRR* for this pair of initial conditions in the Poincaré section is calculated by dividing half of the total number of crossings by the period number: $SRRR_{(1,2)} = -\frac{1}{2}$. This procedure is repeated by shifting both plots, one at a time, n times $\tau^{(1)}$, where $n = 1, 2, \dots, \tau/\tau^{(1)}$ (4 in this case). Since these indexes are symmetrical and $SRRR_{(i,i)} = 0$ by definition, 6 out of 16 initial conditions must be analyzed. (b) $SRRR_{(1,3)} = -\frac{1}{4}$, (c) $SRRR_{(1,4)} = -\frac{1}{2}$, (d) $SRRR_{(2,3)} = -\frac{1}{2}$, (e) $SRRR_{(2,4)} = -\frac{1}{4}$, (f) $SRRR_{(3,4)} = -1/2$. The topological index is displayed by noting the number of times each case is repeated (as exponential numbers) $SRRR_{4_2} = (-\frac{1}{2})^8(-\frac{1}{4})^4 0^4$, or in a simplified notation (“reducing the exponents”): $SRRR_{4_2} = (-\frac{1}{2})^2(-\frac{1}{4})^0$.

TABLE I. Self-relative rotation rates for both the averaged system and the complete system using different numbers of units.

Orbit	$(\omega_0^{(1)}, K_{12})$	$N \rightarrow \infty$	$N = 3000$	$N = 2000$	$N = 1000$	$N = 500$
2 ₁	(5.18, 2.79)	$-\frac{1}{2}0$	$-\frac{1}{2}0$	$(-\frac{1}{2})^3 0$	$(-\frac{1}{3})^4 (-\frac{2}{3})^2 (0)^3$	Non periodic
3 ₁	(5.64, 2.57)	$(-\frac{1}{3})^2 0$	$(-\frac{1}{3})^2 0$	$(-\frac{1}{3})^2 0$	$(-\frac{1}{4})^3 0$	$(-\frac{1}{4})^3 0$
3 ₂	(5.00, 3.21)	$(-\frac{2}{3})^2 0$	$(-\frac{2}{3})^2 0$	$(-\frac{2}{3})^4 0$	$-\frac{1}{2}0$	$-\frac{1}{2}0$
4 ₁	(5.00, 1.88)	$(-\frac{1}{4})^3 0$	$(-\frac{1}{4})^3 0$	$(-\frac{1}{5})^4 0$	Period 6	Non periodic
4 ₂	(5.35, 2.8532)	$(-\frac{1}{2})^2 - \frac{1}{4}0$	$(-\frac{1}{2})^2 - \frac{1}{4}0$	Non periodic	Non periodic	Non periodic
4 ₃	(5.40, 3.32)	$(-\frac{1}{2})^2 - \frac{3}{4}0$	$(-\frac{1}{2})^2 - \frac{3}{4}0$	$-\frac{1}{2}0$	$-\frac{1}{2}0$	$-\frac{1}{2}0$
5 ₁	(5.43, 1.85)	$(-\frac{1}{5})^4 0$	$(-\frac{1}{5})^4 0$	$(-\frac{1}{4})^4 - \frac{1}{2}0$	Non periodic	Non periodic
5 ₂	(5.60, 2.90)	$(-\frac{2}{5})^4 0$	$(-\frac{2}{5})^4 0$	$(-\frac{2}{5})^4 0$	$(-\frac{1}{3})^2 0$	$(-\frac{1}{3})^2 0$

periodic orbits, however, were present in our simulations. The topology of those coincides with the orbits of the same periods in the averaged system, yet they are found at different parameter values (see first row, last column in Table I),

The system of $N=1000$ also presents non periodic orbits at parameter values where the infinite system displays periodicity (see column 6, rows 5 and 7). Also in this case,

we found periodic solutions. The period 2, 3, and 4 solutions of the $N=1000$ set of oscillators have the same topology as their infinite counterpart. For this number of units, we encounter solutions of higher period as well.

Progressive changes are found using $N=2000$ (see column 5 in Table I), but it is for $N=3000$ that we found an equivalence between the finite set and the infinite limit case.

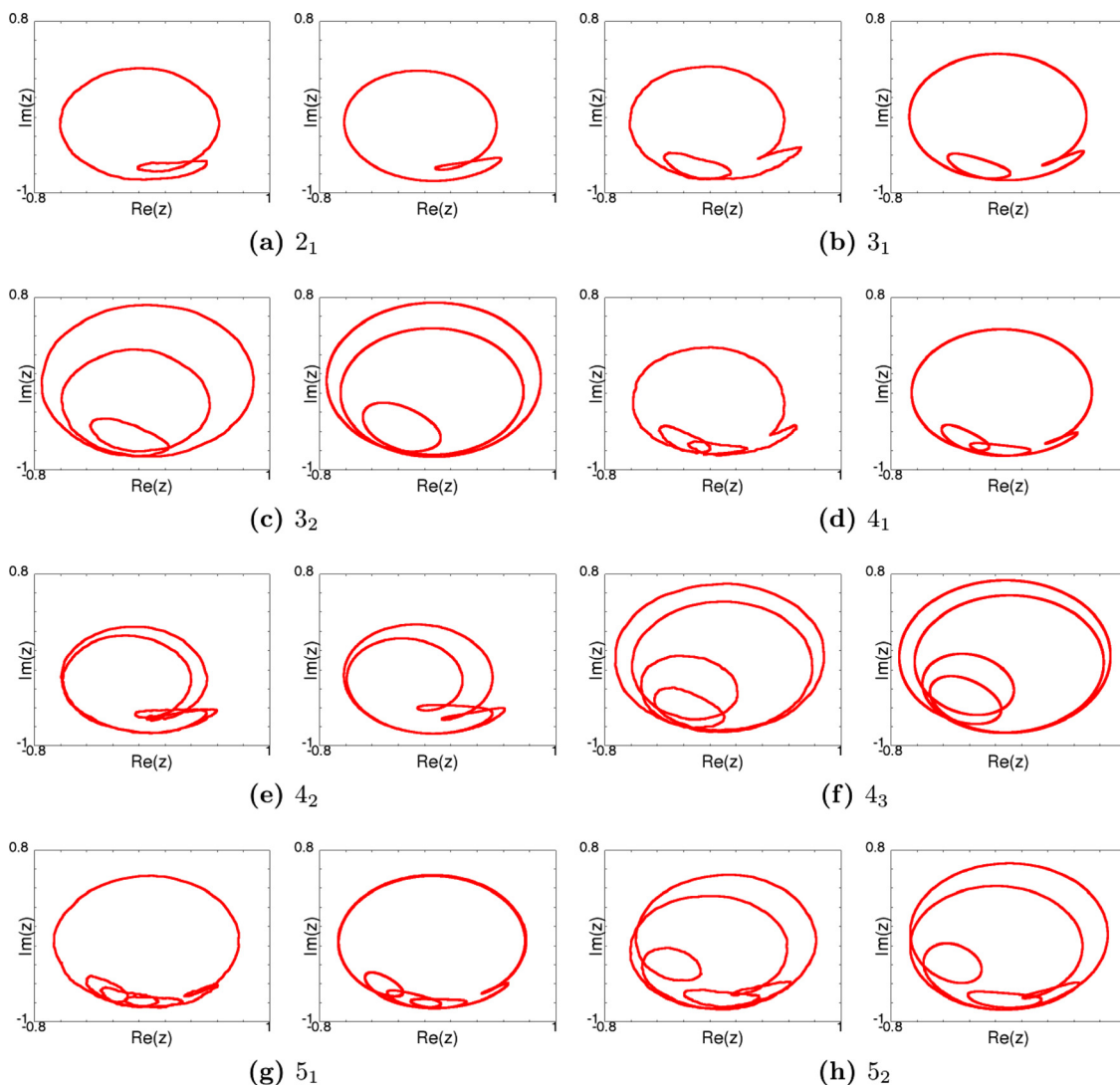


FIG. 3. Comparison of the evolution of the order parameter for both the averaged system (right) and the finite system with $N = 3000$ (left) for each analyzed orbit.

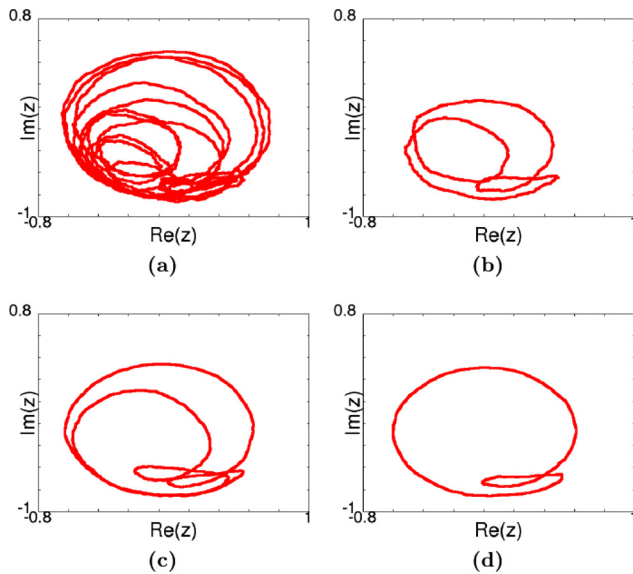


FIG. 4. Dynamics of the order parameter for $(\omega_0^{(1)}, K_{12}) = (5.18, 2.79)$ using different numbers of excitatory units. (a) For $N = 500$, a non periodic structure is found. (b) For $N = 1000$, a 3-period orbit is displayed and (c) for $N = 2000$, a 4-period orbit was found. All these orbits present a different topology than their counterpart in the surrogate system which is achieved for $N = 3000$ (d).

Notice that the first match between the topology of a finite simulation and the infinite limit is achieved for $N = 2000$, where a period five and a period three solutions are equivalent to their counterpart of the infinite set. That match is preserved as N is increased to $N = 3000$. It is likely that once an equivalence is achieved, it will not be lost as N is further increased.

For the finite set of solutions in this study (orbits up to period 5), sets of units larger or equal to 3000 present the same topology as the solutions of the infinitely large system. Beyond the matches between the indexes of the infinite set and the numerically simulated finite system of 3000 elements, in Figure 3, we show the projection of the solutions in two dimensions. Solutions of period 2, 3, 4, and 5 are

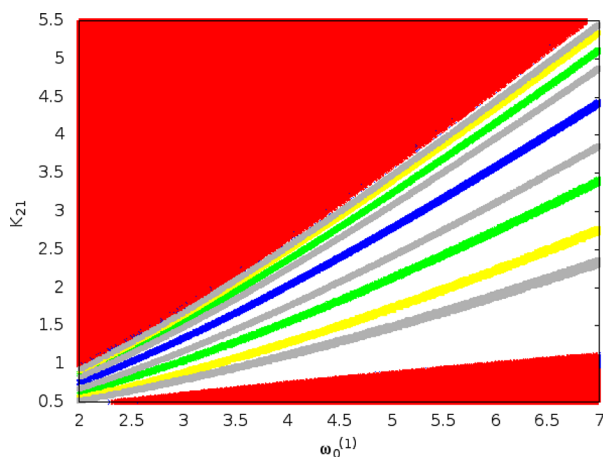


FIG. 5. Arnold tongues diagram for the 3D-system using $\Delta^{(2)} = 0.019$. From bottom to top: A period 5 orbit tongue in gray (named S_1), a period 4 orbit tongue in yellow (4_1) followed by a green tongue (period 3, 3_1) and another period five tongue (5_2). A central period 2 orbit in blue (2_1) is preceded by a zone with two period 5 tongues (5_3 lower and 5_4 higher) and two tongues with period 3 and 4 (3_2 and 4_2).

displayed in (a), (b), (c), (d), (e), (f), (g), and (h), respectively. In all cases, the solutions of the infinite system correspond to the right part of the figure. On the other hand, small sets present solutions that are topologically inequivalent to the ones displayed by the infinite set. In Figure 4, we show a non periodic trajectory for parameter values at which the infinite set presents a period 2 solution (a). For $N = 1000$, and $N = 2000$, periodic solutions are found but yet, of a different periodicity (b) and (c).

It is interesting to explore the role of $\Delta^{(2)}$ in these results, since it describes the dispersion of the parameters of the coupled units being driven. If all units present similar features (i.e., $\Delta^{(2)}$ small), it is reasonable to expect synchronization among the units, which will behave as one unit with its parameters corresponding to the median of the distribution (assuming $\omega_0^{(2)}$ meets the excitability condition). On the contrary, large values of $\Delta^{(2)}$ might lead to a more complex scenario, with many units presenting autonomous oscillations and many other units displaying autonomous excitability.

In order to test this hypothesis, we performed a systematic study, where different populations of units were driven. In each of the numerical experiments, the driven population was chosen to present parameters compatible with distributions of different $\Delta^{(2)}$ values. Here, we present results for values of $\Delta^{(2)}$ smaller than 1 (the value chosen for the population described above) and values of $\Delta^{(2)}$ larger than 1. For large $\Delta^{(2)}$ values, the system presents simple dynamics (period 1), both in the simulation of a large set of units, as well as, in the numerical exploration of the equations describing the average dynamics in the infinite limit. The values explored were $\Delta^{(2)} = 2.0$, $\Delta^{(2)} = 4.3$, and $\Delta^{(2)} = 18.2$, corresponding to 40%, 30%, and 0.1% of the units displaying excitability before being driven, respectively.

For smaller values of $\Delta^{(2)}$, we recovered a complex structure of subharmonic responses in the analyzed region of the $(\omega_0^{(1)}, K_{12})$ parameter space (see Figure 5). We analyzed numerically populations with $\Delta^{(2)} = 0.019$ and $\Delta^{(2)} = 0.168$, which correspond to 90.13% and 60.04% of the units displaying excitability before being forced. The results are summarized in Tables II and III.

TABLE II. Self-relative rotation rates for both the averaged system and the complete system using different numbers of units. In this case, we set $\Delta^{(2)} = 0.019$ in order to have 90.13% excitable units in the uncoupled system.

Orbit	$(\omega_0^{(1)}, K_{12})$	$N \rightarrow \infty$	$N = 3000$	$N = 2000$	$N = 1000$	$N = 500$
2_1	(5.60, 3.26)	$-\frac{1}{2}0$	$-\frac{1}{2}0$	$-\frac{1}{2}0$	$-\frac{1}{2}0$	$-\frac{1}{2}0$
3_1	(6.99, 3.40)	$(-\frac{1}{3})^20$	$(-\frac{1}{3})^20$	$(-\frac{1}{3})^20$	$(-\frac{1}{3})^20$	$(-\frac{1}{3})^20$
3_2	(6.21, 4.36)	$(-\frac{2}{3})^20$	$(-\frac{2}{3})^20$	$(-\frac{2}{3})^40$	$(-\frac{2}{3})^40$	$(-\frac{2}{3})^40$
4_1	(5.19, 1.82)	$(-\frac{1}{4})^30$	$(-\frac{1}{4})^30$	$(-\frac{1}{4})^30$	$(-\frac{1}{4})^30$	$(-\frac{1}{4})^30$
4_2	(6.05, 4.405)	$(-\frac{3}{4})^30$	$(-\frac{3}{4})^30$	$(-\frac{3}{4})^30$	$(-\frac{2}{3})^30$	$(-\frac{2}{3})^30$
5_1	(6.95, 2.31)	$(-\frac{1}{5})^40$	$(-\frac{1}{5})^40$	$(-\frac{1}{5})^40$	$(-\frac{1}{5})^40$	$(-\frac{1}{5})^40$
5_2	(6.95, 3.82)	$(-\frac{2}{5})^40$	$(-\frac{2}{5})^40$	$(-\frac{2}{5})^40$	$(-\frac{2}{5})^40$	Period 8
5_3	(6.95, 4.83)	$(-\frac{3}{5})^40$	$(-\frac{3}{5})^40$	Period 7	Period 9	Period 11
5_4	(6.95, 5.40)	$(-\frac{4}{5})^40$	$(-\frac{4}{5})^40$	$(-\frac{3}{4})^30$	Period 7	Non periodic

TABLE III. Self-relative rotation rates for both the averaged system and the complete system using different numbers of units. In this case, we set $\Delta^{(2)} = 0.1675$ in order to have 60.04% excitable units in the uncoupled system.

Orbit	$(\omega_0^{(1)}, K_{12})$	$N \rightarrow \infty$	$N = 3000$	$N = 2000$	$N = 1000$	$N = 500$
2 ₁	(5.60, 3.26)	$-\frac{1}{2}0$	$-\frac{1}{2}0$	$-\frac{1}{2}0$	Period 9	Period 7
3 ₁	(6.99, 3.40)	$(-\frac{1}{3})^2 0$	$(-\frac{1}{3})^2 0$	$(-\frac{1}{3})^2 0$	$(-\frac{1}{3})^2 0$	Non periodic
3 ₂	(6.21, 4.36)	$(-\frac{2}{3})^2 0$	$(-\frac{2}{3})^2 0$	$(-\frac{2}{3})^4 0$	Period 7	Period 7
4 ₁	(5.19, 1.82)	$(-\frac{1}{4})^3 0$	$(-\frac{1}{4})^3 0$	$(-\frac{1}{4})^3 0$	$(-\frac{1}{4})^3 0$	Period 6
4 ₂	(6.05, 4.405)	$(-\frac{3}{4})^3 0$	$(-\frac{3}{4})^3 0$	Period 16	$(-\frac{2}{3})^3 0$	Period 8
5 ₁	(6.95, 2.31)	$(-\frac{1}{5})^4 0$	$(-\frac{1}{5})^4 0$	$(-\frac{1}{5})^4 0$	$(-\frac{1}{5})^4 0$	Period 6
5 ₂	(6.95, 3.82)	$(-\frac{2}{5})^4 0$	$(-\frac{2}{5})^4 0$	$(-\frac{2}{5})^4 0$	$(-\frac{1}{3})^2 0$	$(-\frac{1}{3})^2 0$
5 ₃	(6.95, 4.83)	$(-\frac{3}{5})^4 0$	$(-\frac{3}{5})^4 0$	Period 7	Period 15	Period 23
5 ₄	(6.95, 5.40)	$(-\frac{4}{5})^4 0$	$(-\frac{4}{5})^4 0$	$(-\frac{3}{4})^3 0$	Non periodic	$(-\frac{2}{3})^2 0$

As in the example described above ($\Delta^{(2)} = 1$, resulting on a rate of 46.53% of the units presenting excitability), we compared the topological features of the average system computed by simulating the coupling between N units, with the topology of the solutions of the equations describing the averaged dynamics in the infinite limit. As expected, when the system is more homogeneous, it is easy to reach synchronization among the units, and, therefore, with a smaller number of coupled units, the system behaves as the infinite limit problem.

In the case of $\Delta^{(2)} = 0.168$, for $N = 500$, none of the orbits present the same topology as the averaged system. For $N = 2000$, all the studied orbits but three behave as the infinite limit approximation. In the case of $\Delta^{(2)} = 0.019$, for $N = 2000$, only two orbits have not yet recovered the topology of the infinite limit. In this case with as low as $N = 500$, we get four orbits with the same topology as the infinite case.

In summary, the dispersion of the parameters correlates with the number of units necessary to use in order to recover the average properties of an infinite-sized system.

IV. DISCUSSION AND CONCLUSIONS

In the last few years, there were important advances in the understanding of large systems of globally coupled phase oscillators. Particularly helpful in this program was the study of the infinite size limit: A surrogate problem where, instead of a large number of units, one studies the average properties of a set of size infinity. In a variety of problems where the units are coupled sinusoidally,^{7,13} in this limit, the dynamics was found to display low dimensional behavior.

We used topological tools to compare the low dimensional dynamics presented on average by a large system of coupled forced excitable units, with the behavior of its infinite size surrogate system.

In order to do so, we studied numerically different sets of coupled, forced excitable units, and found that $N = 3000$ units were enough to obtain the same topological structure of the flow than in the infinite size problem. To establish this equivalence, we looked up the topological organization of periodic orbits of period five and lower. The rationale behind requesting equivalence for orbits of low period is that

experimentally, it is difficult to reconstruct the topological features of higher periodic orbits.¹⁸ Moreover, it has been shown that optimal orbits in flows are found in lower periods.¹⁹ In any case, the pertinence of approximating a finite set with its infinite size surrogate will depend on the experimental situation.

In this work, for the explored range of parameters, we found that the dynamics of a few thousand of driven, coupled, excitable units can be adequately approximated by a surrogate of infinite size. This allows us to work with a low dimension system, describing its averaged dynamics, capable of reflecting the same features as the finite system. For different problems, and specially depending on the studies of their orbits, the number of units of the finite set that can be approximated in this way will change. Solutions displaying branches that live closely in the phase space are likely to demand a larger N to be well approximated by the solutions of the infinite system. We also found in our numerical explorations that the larger the parameter dispersion, the larger the number of units are necessary to achieve the features found in the infinite system surrogate. This work presents a rigorous strategy to deal with the pertinence of approximating finite sets by infinitely large ones.

ACKNOWLEDGMENTS

This work was supported by Conicet and the University of Buenos Aires.

¹A. T. Winfree, *Geometry of Biological Time*, 1st ed. (Springer, 1980).

²Y. Kuramoto, *Chemical Oscillations, Waves, and Turbulence* (Springer, 1984).

³A. Pikovsky, M. Rosenblum, and J. Kurths, *Synchronization: An Universal Concept in Nonlinear Sciences* (Cambridge University Press, 2001).

⁴E. Ott and T. M. Antonsen, *Chaos* **18**, 037113 (2008).

⁵L. M. Childs and S. H. Strogatz, *Chaos* **18**, 043128 (2008).

⁶T. M. Antonsen, R. T. Faghih, M. Girvan, E. Ott, and J. Platig, *Chaos* **18**, 037112 (2008).

⁷L. M. Alonso and G. B. Mindlin, *Chaos* **21**, 023102 (2011).

⁸G. B. Mindlin, X. Hou, H. Solari, R. Gilmore, and N. B. Tuffillaro, *Phys. Rev. Lett.* **64**(20), 2350 (1990).

⁹G. B. Mindlin, R. Lopez-Ruiz, R. Gilmore, and H. Solari, "Horseshoe implications," *Phys. Rev. E* **48**, 4297 (1993).

- ¹⁰R. Gilmore and M. Lefranc, *The Topology of Chaos* (Wiley, Hoboken, 2002).
- ¹¹L. M. Alonso, J. A. Alliende, and G. B. Mindlin, *Eur. Phys. J. D* **60**(2), 361 (2010).
- ¹²P. So and E. Barreto, *Chaos* **21**, 033127 (2011).
- ¹³P. So, T. B. Luke, and E. Barreto, *Physica D* **267**, 16 (2014).
- ¹⁴T. Yang, B. R. Hunt, and E. Ott, *Phys. Rev E* **62**, 1950 (2000).
- ¹⁵P. S. Skardal, D. Taylor, and J. G. Restrepo, *Physica D* **267**, 27 (2014).
- ¹⁶G. Barlev, T. M. Antonsen, and E. Ott, *Chaos* **21**, 025103 (2011).
- ¹⁷H. G. Solari and R. Gilmore, *Phys. Rev. A* **37**, 3096–3109 (1988).
- ¹⁸G. B. Mindlin, H. G. Solari, M. A. Natiello, R. Gilmore, and X. Hou, *J. Nonlinear Sci.* **1**(2), 147 (1991).
- ¹⁹T. H. Yang, B. R. Hunt, and E. Ott, *Phys. Rev. Lett.* **62**(2), 1950 (2000).